

High-resolution and high-fidelity x-ray mask structure employing embedded absorbers

S. Y. Chou, N. I. Maluf, and R. F. W. Pease

Stanford Solid State Electronics Laboratory, Stanford University, Stanford, California 94305

(Received 20 July 1988; accepted 24 August 1988)

Existing x-ray masks often suffer from a variety of problems. These include poor adhesion of small absorber features to the substrate, severe undercut in the etching of sub-half-micron absorber lines, distortion of absorbing features formed by plating through a resist stencil, distortion of the absorber due to metal migration and due to local stress, and mechanical damage due to handling. Here we describe an x-ray mask structure in which a high atomic number metal fills trenches etched into a single-crystal silicon mask membrane. Thus the problems mentioned earlier for conventional x-ray masks can be either effectively eliminated or greatly reduced. The trenches were formed in the silicon by a combination of ultrathin resist, high-resolution electron beam exposure, and novel etching techniques involving metal masking. The trenches were half-micron deep with a sidewall angle of 1.5° to the vertical, and the minimum trench width measured at the top of the trenches was 70 nm, which gives an aspect ratio of 7:1. The trenches were filled with tungsten by both selective and nonselective chemical vapor deposition, and back etching (if any) was performed using reactive ion etching. Scanning electron microscopy reveals that the tungsten features are faithful replicas of the vertically walled trenches. A one-dimensional stress model shows that for a finite absorber stress, the embedded mask can have zero in-plane distortion and an out-of-plane distortion that is much less than that in a conventional mask.

I. INTRODUCTION

X-ray mask technology has become recognized as the most critical aspect of x-ray lithography. In a conventional x-ray mask structure, as shown in Fig. 1 (a), x-ray absorbers are on a surface of a mask membrane. This mask structure suffers a variety of problems. First, the adhesion between a small absorber feature and the mask membrane is often poor due to the small contact area, and therefore small absorber features can separate from the membrane. Second, it is difficult to control the linewidth of the absorbers with a high precision, either when the absorbers are patterned subtractively by an etching technique,¹ or when the absorbers are patterned additively, by electroplating through a resist stencil.² Third, the stress of an absorber can distort the mask. Fourth, the width of a narrow free standing absorber can change due to metal migration.³ Fifth, the mask with high aspect ratio absorbers cannot be cleaned with solvent, because the surface tension of liquid between two adjacent upright absorbers can bend or peel the absorbers off the membrane.⁴ Finally, the absorber extending above the membrane surface is susceptible to mechanical damage, and dust lodged in the gap between adjacent absorber lines is hard to remove.

Jones *et al.*⁵ and Wada *et al.*⁶ suggested a mask structure in which a layer of an x-ray transparent material is coated on the top of the absorber of a conventional mask. This mask structure can solve some of the problems mentioned earlier. Kawabuchi suggested another x-ray mask structure in which an amorphous insulating material stencil (say, silicon dioxide, boron nitride, and the like) is put on the top of a conducting x-ray mask membrane, then gold or platinum is electroplated through openings of the stencil, and the stencil will not be removed.⁷ Although this mask structure can improve many of the problems mentioned earlier, the thick amorphous stencil layer adds a lot of stress to the mask mem-

brane. This additional stress might offset the advantages that the mask structure brings. The embedded mask structure described here can either effectively eliminate or greatly reduce the above problems.

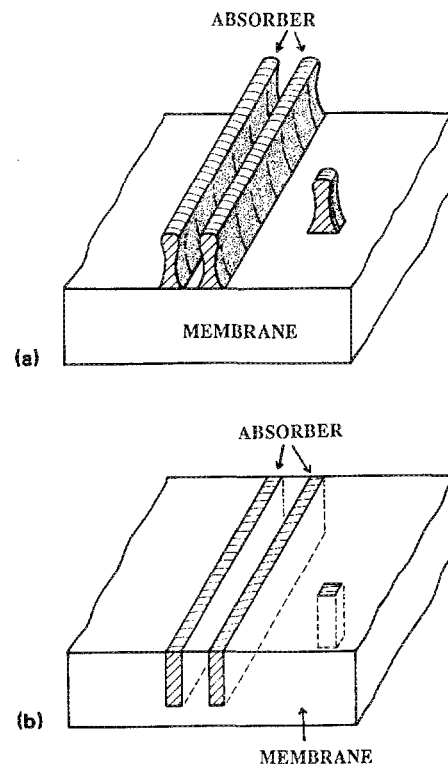


FIG. 1. The schematic of (a) a conventional x-ray mask and (b) an embedded x-ray mask.

II. MASK STRUCTURE AND FABRICATION

The x-ray mask structure consists of a single-crystal membrane patterned in the form of trenches that are filled with metal absorber [Fig. 1(b)].

The four main steps in the fabrication of the embedded mask are (i) mask pattern definition, (ii) reactive ion etching (RIE) of the trenches in single-crystal Si, (iii) trench filling using chemical vapor deposition, and (iv) thinning to form the silicon membrane (Fig. 2).

The wafers used are *n*-type (100) silicon with a resistivity of 5 Ω cm. The surfaces of the wafer are doped with boron by diffusion at 1000 °C for 3 h in a BBr₃ source. An oxide of 100-nm thickness is then thermally grown. The trenches are formed in the Si by two methods. In the first method, a layer of Cr of 50-nm thickness is electron beam (e-beam) evaporated on the front surface, followed by a 14.3-nm-thick poly(methylmethacrylate) (PMMA) (17 monolayers) deposited using the Langmuir-Blodgett technique.⁸ Exposure is performed using an ultrahigh resolution e-beam system.⁹ The PMMA patterns are transferred to Cr by a chemical etch in Cyantek CR-14 for 30 s, then to the underlying SiO₂ using reactive ion etching. After removing the PMMA, reactive ion etching in Cl₂/SiCl₄/N₂ gases forms 0.5- μ m-deep trenches in the silicon membrane, and Cr is removed afterwards. The details of thin resist, e-beam lithography and the trench etching will be published elsewhere.¹⁰ In the second method a layer of AZ1370 of 1- μ m thickness is spun on the oxide and patterned using optical lithography. The pattern is then transferred into SiO₂ using reactive ion etching. After removing the resist, reactive ion etching in Cl₂/SiCl₄/N₂ gases form 0.5- μ m-deep trenches in the silicon membrane.

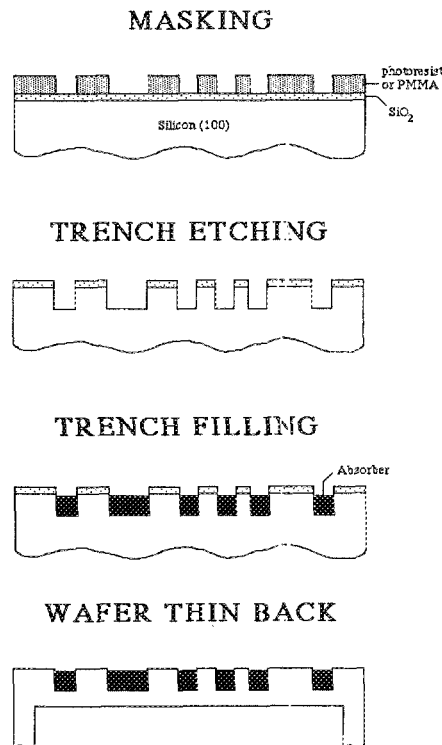


FIG. 2. Schematic of main steps in fabricating the embedded mask.

The trenches are filled with tungsten by either selective deposition or nonselective chemical vapor deposition (CVD) followed by etch-back. The deposition temperature and pressure were 580 °C and 400 mTorr for the selective process, and 300 °C and 200 mTorr for the nonselective process, respectively. Both depositions were performed in a WF₆ and H₂ gas mixture. Finally, SiO₂ is removed, and ethylene-diamine-pyrocatechol is used to etch the silicon from the back, leaving a membrane of 3- μ m thickness and 2-cm diameter. The boron doped surface acts as an etch stop to form the membrane.

III. RESULTS

Figure 3 shows a trench formed by the first method in an undoped silicon substrate. It is 0.5 μ m deep, and has a top opening 70 nm wide and a bottom opening 40 nm wide. Thus the sidewall of the trench is 1.5° from the vertical, and the aspect ratio is 7:1. The etching is repeatable and there is no significant difference in etch rate or vertical angle for undoped and boron doped silicon.¹⁰

Figure 4 shows a silicon trench completely filled with tungsten by selective deposition. The trench is formed by the second method described earlier. The sidewall is 5° off the vertical, which is more than twice as large as that etched with a Cr mask. As noticed, RIE etching of Si without a Cr mask also creates two grooves of 40-nm width at corners of the trench; nonetheless, the CVD deposition of tungsten can fill these small grooves perfectly. Furthermore, even when tungsten is deposited simultaneously on all three walls of the trench, there is no void formed in the tungsten. Tungsten spills over the trench, and was back-etched afterwards using RIE in SF₆ as shown in Fig. 5. Figure 6 shows a via of 0.6- μ m diameter filled with tungsten. We also observed that in nonselective CVD deposition, if the deposited tungsten is thicker than the width of a trench then the top surface of the tungsten is essentially flat. Therefore, a maskless etching can remove unwanted tungsten.

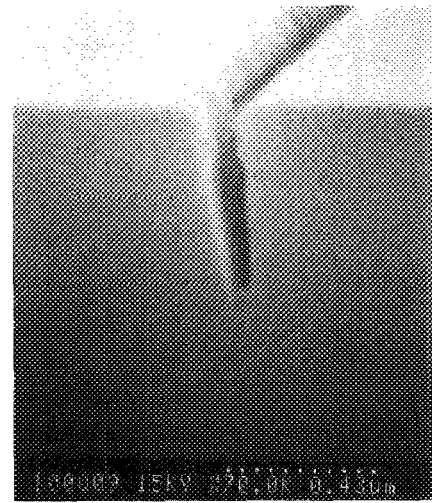


FIG. 3. A trench of a width of 70 nm and depth of 0.5 μ m etched into an undoped Si by using e-beam lithography, thin resist, and RIE.

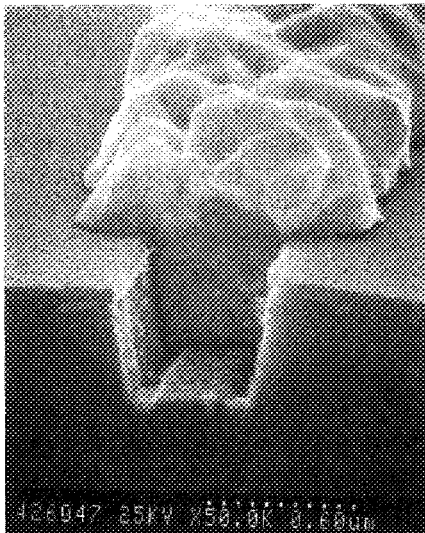


FIG. 4. A trench filled with tungsten before etch-back. The trench is etched into undoped Si using optical lithography and RIE.

IV. DISCUSSION

The embedded mask structure has many advantages over the conventional mask. In the embedded x-ray mask structure, the absorber not only has larger contact area to the mask membrane than that in a conventional mask, also, it has the additional mechanical support from the sidewalls and is bounded by the membrane. Therefore, this mask structure avoids the problems associated with poor adhesion, metal migration, and surface tension of liquid; and it is robust to mechanical damage of the absorbers.

Another advantage of this mask is that present technology allows us to pattern sub-quarter-micron trenches of high aspect ratio in single-crystal silicon with a sufficient accuracy.

The embedded mask structure also relaxes the requirement of mechanical strength of an absorber, so that many high atomic number metals such as rare-earth metals or even

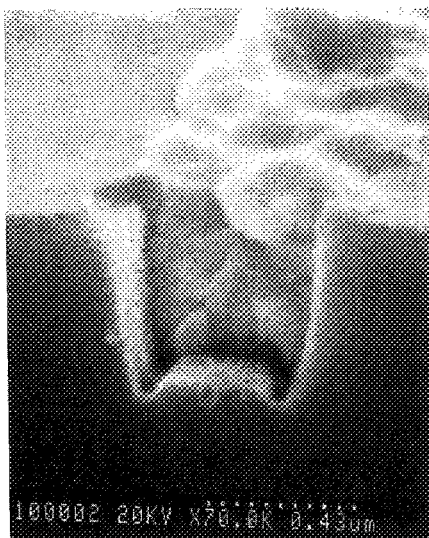


FIG. 5. A trench similar to the Fig. 4 filled with tungsten after etch-back.

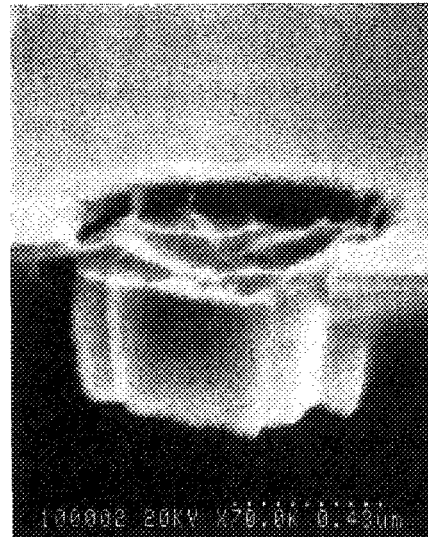


FIG. 6. A via of 0.6- μm diameter filled with tungsten.

liquid metals can be used as an absorber. This freedom of choosing a variety of absorbers can result in increasing mask contrast (for a given absorber thickness) or minimizing mask distortion caused by the stress. For example, uranium-238 has an absorption coefficient almost twice as much as that of gold. Another example is that lead has an elastic modulus 23 times less than that of tungsten, and a shear modulus 27 times less.

For a finite absorber stress, a one-dimensional stress model predicts that the embedded mask can have zero in-plane distortion, and an out-of-plane distortion which is much smaller than that in a conventional mask. In-plane distortion (IPD) occurs in a conventional mask, whenever the stress of the absorber is nonzero. The tensile stresses in membrane under the absorber σ'_m and outside absorber σ_m , and the tensile stress in absorber σ_a , in equilibrium have to satisfy the following relation¹¹:

$$\sigma'_m t_m = \sigma_m t_m + \sigma_a t_a,$$

where t_m and t_a are the thicknesses of membrane and absorber, respectively. Thus the membrane is relatively compressed under the absorber and relatively stretched outside the absorber.

However, for the embedded mask, we have an extra degree of freedom in control of the membrane stress by choosing the depth of the trench etched in the membrane, t_t , as depicted in Fig. 7. Then in the equilibrium the stresses in an embedded mask satisfy

$$\sigma'_m t_m = \sigma_m (t_m - t_t) + \sigma_a t_a.$$

Thus for finite absorber stress and thickness, the IPD in the one-dimensional model becomes zero (i.e., $\sigma'_m = \sigma_m$, assuming the boundary of the membrane is fixed) as long as

$$t_t = (\sigma_a / \sigma_m) t_a. \quad (1)$$

The out-of-plane distortion (OPD) of a mask can be described by downward deflection of the membrane η as shown in Fig. 8. The deflection at the absorber edge for a conventional mask is given by¹¹

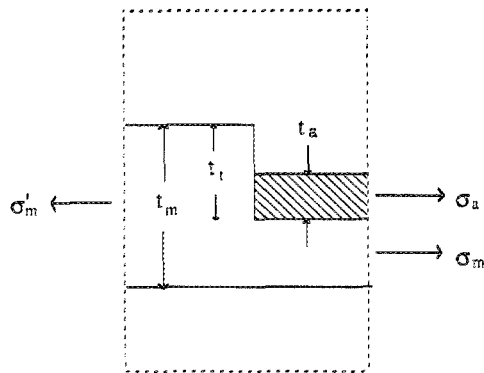


FIG. 7. Schematic of the stresses in an embedded mask.

$$\eta_0^{\text{con}} = \frac{\sigma_a t_a (t_m + t_a)}{4\sigma'_m t_m} D,$$

where D is the stiffness of the membrane to bending.

Using a similar model to that in Ref. 11, the deflection of the membrane at the absorber edge for an embedded mask is given by

$$\eta_0^{\text{em}} = \frac{\sigma_a t_a (t_m - t_i + t_a) - \sigma'_m t_m t_i}{4\sigma'_m t_m} D.$$

Therefore the ratio of the two deflections for the same absorber thickness and the same membrane thickness is

$$\begin{aligned} \frac{\eta_0^{\text{em}}}{\eta_0^{\text{con}}} &= \frac{(t_m - t_i + t_a) - (\sigma'_m t_m / \sigma_a t_a) t_i}{t_m + t_a} \\ &= 1 - \frac{t_i + (\sigma'_m t_m / \sigma_a t_a) t_i}{t_m + t_a}. \end{aligned} \quad (2)$$

The second term in the equation is positive, so $\eta_0^{\text{em}}/\eta_0^{\text{con}} < 1$, namely, the OPD, is smaller in the embedded mask.

Using the condition for zero IPD, i.e., Eq. (1), Eq. (2) becomes

$$\frac{\eta_0^{\text{em}}}{\eta_0^{\text{con}}} = 1 - \frac{t_m + t_i}{t_m + t_a}. \quad (3)$$

This equation shows that if the stress of the absorber is the same as that of the membrane, then $t_i = t_a$, and the embedded mask should have zero IPD and zero OPD. It also shows that if the trench depth is larger than the absorber thickness, then the membrane is deflected in the opposite direction.

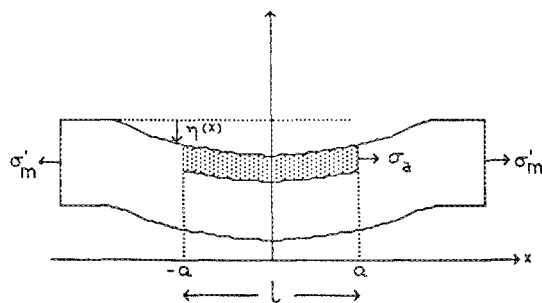


FIG. 8. Schematic of out-of-plane distortion in a membrane due to a one-dimensional feature.

Let us apply Eq. (3) to a practical case. Assume, $2\sigma'_m = \sigma_a$, $t_m = 4t_a$. For zero IPD, it requires, using Eq. (1), $t_i = 2t_a$. Thus Eq. (3) becomes

$$\left| \frac{\eta_0^{\text{em}}}{\eta_0^{\text{con}}} \right| = \left| 1 - \frac{4t_a + 2t_a}{4t_a + t_a} \right| = 0.2,$$

which indicates that the OPD in the embedded mask is five times smaller.

Although the distortion in a real mask is different from the one-dimensional model, the one-dimensional model illustrates the possibilities for reducing distortion by employing the embedded structure and controlling the depth of fill of the trenches.

The above discussion also illustrates why thinning the silicon membrane is the last step, instead of the first as in conventional mask making. When the trenches are etched in Si, they generate some additional local stress. However, the stress will not cause any significant distortion, because the silicon substrate is much thicker than the depth of a trench. Deposition of the absorber will balance the stress caused by the trenches. Therefore, the distortion will be minimized, if formation of a membrane is the last step of the fabrication. Certainly, the above argument assumes that the doping in the remaining silicon substrate is uniform and that the silicon thinning results in a very uniform and smooth back-surface.

Thermal expansion of silicon and tungsten are different. This means that in order to control the mask distortion, the mask working temperature has to be well controlled.

V. SUMMARY

We have proposed and fabricated an x-ray mask structure, in which a high atomic number metal fills trenches etched in the single-crystal Si membrane. This mask structure should allow us to reduce some of the problems suffered by a conventional x-ray mask. The trenches are formed in Si substrate by using ultrahigh resolution e-beam lithography, ultrathin resist, Cr mask layer, and reactive ion etching. The trenches were a half-micron deep with a sidewall angle of 1.5° to the vertical; and the minimum trench width measured at the top of the trenches was 70 nm, which gives an aspect ratio of 7:1. The trenches were filled with tungsten by both selective and nonselective chemical vapor deposition. Scanning electron microscopy reveals that the tungsten in the trenches is void-free, so that the absorber features are faithful replicas of the vertically walled trenches, when etch-back is successfully accomplished. A one-dimensional stress model predicts that for a finite absorber stress, the embedded mask can have zero in-plane distortion, and an out-of-plane distortion much smaller than that in a conventional mask.

ACKNOWLEDGMENTS

We would like to thank S. W. J. Kuan for preparation of the LB film, D. R. Allee for ultrahigh resolution e-beam lithography, Paul Jerabek for MEBES writing, J. McVittie of Stanford I. C. Laboratory, H. E. T. Gaw, D. Seligson, J. Carruthers of Intel for useful discussions, and Genus Inc. for some of tungsten deposition. The work was supported by grants from Intel and Hampshire Instruments.

- ¹See, for example, J. N. Randall and J. C. Wolfe, *Appl. Phys. Lett.* **39**, 742 (1981); I. Plotnik, M.S. thesis, MIT, 1985.
- ²M. L. Schattenburg (private communication).
- ³R. C. Jaklevic and L. Elie, *Phys. Rev. Lett.* **60**, 120 (1988).
- ⁴M. L. Schattenburg, Ph.D. thesis, MIT, 1984.
- ⁵A. B. Jones and S. G. Plonski, U.S. Patent No. 4 536 882 (20 August 1985).
- ⁶T. Wada, S. Sakurai, and K. Kawabuchi, *J. Vac. Sci. Technol.* **19**, 1208 (1981).
- ⁷K. Kawabuchi, U.S. Patent No. 4 451 544 (29 May 1984).
- ⁸K. B. Blodgett, *J. Am. Chem. Soc.* **57**, 1007 (1935).
- ⁹T. H. Newman, K. E. Williams, and R. F. W. Pease, *J. Vac. Sci. Technol. B* **5**, 88 (1987).
- ¹⁰N. I. Maluf, S. Y. Chou, S. Kuan, D. Allee, and R. F. W. Pease, *J. Vac. Sci. Technol.* (submitted).
- ¹¹A. W. Yanof, D. J. Restnick, C. A. Jankoski, and W. A. Johnson, *SPIE* **632**, 118 (1986).